



Title	A geometrical approach to robust minimum variance beamforming
Author(s)	Wong, N; Ng, TS; Balakrishnan, V
Citation	Icassp, Ieee International Conference On Acoustics, Speech And Signal Processing - Proceedings, 2003, v. 5, p. 329-332
Issued Date	2003
URL	http://hdl.handle.net/10722/46422
Rights	©2003 IEEE. Personal use of this material is permitted. However, permission to reprint/republish this material for advertising or promotional purposes or for creating new collective works for resale or redistribution to servers or lists, or to reuse any copyrighted component of this work in other works must be obtained from the IEEE.

A GEOMETRICAL APPROACH TO ROBUST MINIMUM VARIANCE BEAMFORMING

Ngai Wong[†], Tung-Sang Ng[†], Venkataramanan Balakrishnan[‡]

[†] Department of EEE, The University of Hong Kong, Pokfulam Road, Hong Kong

[‡] School of ECE, Purdue University, West Lafayette, IN 47907-1285

ABSTRACT

This paper presents a highly efficient geometrical approach for designing robust minimum variance (RMV) beamformers against uncertainties in the array steering vector. Instead of the conventional approach of modeling the uncertainty region by a convex closed space, the proposed algorithm exploits the optimization constraint and shows that optimization only needs to be done on the intersection of a hyperplane and a second-order cone (SOC). The problem can then be cast as a second-order cone programming (SOCP) problem so as to enjoy the high efficiency of a class of interior point algorithms. A general case of modeling the uncertainties of an array using complex-plane trapezoids is investigated. The efficiency and tightness of the proposed method over other schemes are demonstrated with numerical examples.

1. INTRODUCTION

In antenna array design, uncertainties in the steering vector of the desired signal can arise due to a multitude of reasons including array calibration errors, uncertainty in the angle-of-arrival (AOA), array imperfection and environmental inhomogeneities etc. [1]-[4]. The minimum variance (MV) beamformer is an application of the Capon's method [5] that minimizes the variance of the combined array output while maintaining a unity gain towards the look direction. Nonetheless, the performance of this MV beamformer is known to be quite sensitive and susceptible to mismatches in the presumed and actual steering vectors [4].

Recent progress has been made by transforming the robust beamformer design into a programming task [1], [2], [6]. The steering vector is modeled as part of a convex set (the uncertainty region) and optimization is done for all elements within this set. One example is to encompass the uncertainty by a hypersphere around the nominal steering vector [1]. The optimization is then cast as an SOCP problem [7] and solved efficiently via interior point algorithms (e.g., [8], [9]). Simulations have shown the superiority of this approach over other popular robust

beamformers in adaptive arrays [1]. However, a hypersphere derived from the strong worst-case condition does not exploit the structure of the uncertainty, and may sometimes lead to impractical or even infeasible design. Another robust design method is to encompass the uncertainty set by a polyhedral cone [2]. A drawback is that the use of a polyhedral cone with limited extreme rays (the basis rays of a cone) can result in overly conservative constraints as in the previous case, while increasing the number of extreme rays will cause an exponential growth in the problem complexity and prohibit its use in larger arrays. Also, the cone angle determination of the polyhedral cone was not pursued further in [2].

This paper extends the polyhedral cone bounding idea to a second-order cone (SOC) and provides a constructive way to obtain the smallest SOC encompassing the uncertainty convex set. By exploiting the optimization constraint, it is shown that optimization only needs to be done on the intersection of an SOC and a hyperplane *outside* the convex set. The problem can naturally be formulated and solved as an SOCP problem. With numerical examples, the robust minimum variance (RMV) beamformer obtained this way is shown to have accurate uncertainty modeling and favorable power requirement.

2. MINIMUM VARIANCE BEAMFORMING

First, the output $\mathbf{x}(t) \in \mathbb{C}^N$ of an N -element array is

$$\mathbf{x}(t) = \mathbf{a}(\theta)s(t) + \mathbf{A}_1\mathbf{S}_1(t) + \mathbf{n}(t) \quad (1)$$

where $\mathbf{a}(\theta) \in \mathbb{C}^N$ is the steering vector of the desired narrowband signal $s(t)$, \mathbf{A}_1 is an $N \times L$ matrix whose l th column, $\mathbf{a}(\theta_l)$, is the steering vector of the l th interfering signal in $\mathbf{S}_1(t) = [s_1(t) \cdots s_L(t)]^T$, and $\mathbf{n}(t) \in \mathbb{C}^N$ is the additive noise component. The combined output of the array subject to a complex weight \mathbf{w} is

$$y(t) = \mathbf{w}^* \mathbf{x}(t) \quad (2)$$

Here $(\cdot)^*$ denotes conjugate transpose. The interference-plus-noise covariance matrix \mathbf{R}_{in} is defined as

$$\mathbf{R}_{in} = \mathbf{E}((\mathbf{A}_1\mathbf{S}_1(t) + \mathbf{n}(t))(\mathbf{A}_1\mathbf{S}_1(t) + \mathbf{n}(t))^*) \quad (3)$$

whereas the sample covariance matrix \mathbf{R}_x is defined (and

approximated by M recently received samples) as

$$\mathbf{R}_x = \mathbf{E}(\mathbf{x}\mathbf{x}^*) \approx \frac{1}{M} \sum_{p=1}^M \mathbf{x}(p)\mathbf{x}(p)^* \quad (4)$$

A metric for the performance of a beamformer is the signal-to-interference-plus-noise ratio (SINR) defined as

$$\text{SINR} = \frac{|\mathbf{w}^* \mathbf{a}(\theta)|^2}{\mathbf{w}^* \mathbf{R}_x \mathbf{w}} \quad (5)$$

The MV beamformer is obtained by solving

$$\min(\mathbf{w}^* \mathbf{R}_x \mathbf{w}) \text{ subject to } \mathbf{w}^* \mathbf{a}(\theta_p) = 1 \quad (6)$$

where θ_p and $\mathbf{a}(\theta_p)$ are the presumed AOA and steering vector respectively. If this presumed steering vector matches the physical steering vector, we have an optimal solution of (6) given by the Capon's method [5]

$$\mathbf{w}_{mv} = \mathbf{R}_x^{-1} \mathbf{a}(\theta_p) / \mathbf{a}(\theta_p)^* \mathbf{R}_x^{-1} \mathbf{a}(\theta_p) \quad (7)$$

In the presence of steering vector uncertainties, the constraint in (6) is generalized to a gain greater than or equal to unity [1], [2], i.e.,

$$\min(\mathbf{w}^* \mathbf{R}_x \mathbf{w}) \text{ subject to } \text{Re}(\mathbf{w}^* \mathbf{a}) \geq 1, \forall \mathbf{a} \in \Omega \quad (8)$$

where $\text{Re}(\circ)$ and $\text{Im}(\circ)$ (below) give the real part and imaginary parts of its argument and Ω is a set that contains the uncertainties of the steering vector \mathbf{a} . For ease of programming, complex quantities are transformed into real values (indicated by tildes) by defining

$$\tilde{\mathbf{w}} = \begin{bmatrix} \text{Re}(\mathbf{w}) \\ \text{Im}(\mathbf{w}) \end{bmatrix}, \tilde{\mathbf{a}} = \begin{bmatrix} \text{Re}(\mathbf{a}) \\ \text{Im}(\mathbf{a}) \end{bmatrix}, \quad (9)$$

$$\tilde{\mathbf{R}}_x = \begin{bmatrix} \text{Re}(\mathbf{R}_x) & -\text{Im}(\mathbf{R}_x) \\ \text{Im}(\mathbf{R}_x) & \text{Re}(\mathbf{R}_x) \end{bmatrix}$$

such that (8) can be rewritten as

$$\min(\tilde{\mathbf{w}}^T \tilde{\mathbf{R}}_x \tilde{\mathbf{w}}) \text{ subject to } \tilde{\mathbf{w}}^T \tilde{\mathbf{a}} \geq 1, \forall \tilde{\mathbf{a}} \in \tilde{\Omega} \quad (10)$$

where $\tilde{\Omega}$ is an appropriate set derived from Ω .

3. GEOMETRICAL APPROACH

Now suppose we have a set of sample points $\tilde{\Omega} = \{\tilde{\mathbf{a}}_1, \tilde{\mathbf{a}}_2, \dots\}$ whose convex combinations denote the possible values of $\tilde{\mathbf{a}}$. Since the optimization constraint $\tilde{\mathbf{w}}^T \tilde{\mathbf{a}} \geq 1$ in (10) is convex in $\tilde{\mathbf{a}}$, optimization can be performed under a stronger condition, namely, on the vertices or curved boundaries of a convex set that contains $\tilde{\Omega}$ (e.g., see [6]). With reference to Fig. 1, the proposed generic RMV beamforming algorithm is summarized in the following 4 steps:

Step 1. Construct a minimum convex hull of $\tilde{\Omega}$.

Step 2. Fit the smallest SOC around the hull.

Step 3. Intersect the cone with a hyperplane tangent to the bottom of the hull.

Step 4. Optimize (10) with respect to $\tilde{\mathbf{w}}$ on the rim of the hyperellipse resulting from the intersection.

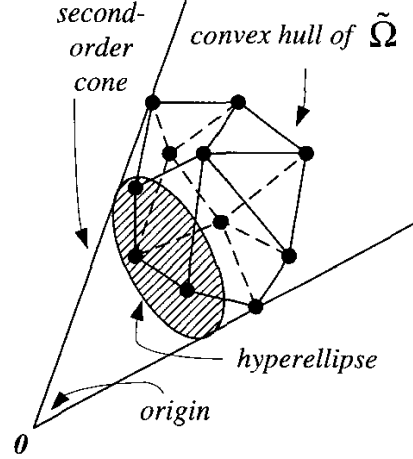


Fig. 1. A second-order cone bounding the convex hull of $\tilde{\Omega}$.

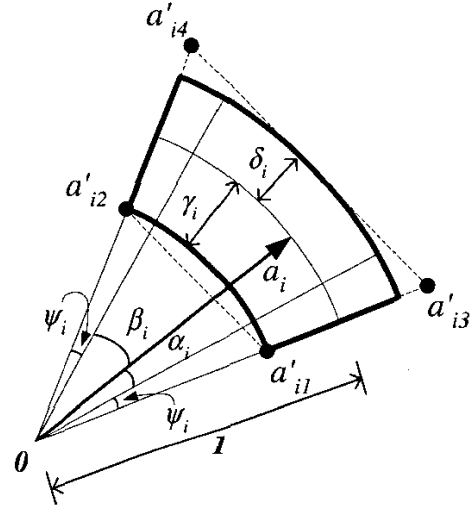


Fig. 2. Uncertainty of a steering vector element (bold annulus sector) bounded in a trapezoid (formed by the 4 dots).

A novelty here is that by convexity, it can be easily proved that if the optimization constraint holds on the rim of the hyperellipse, it is also satisfied for any $\tilde{\mathbf{a}}$ on the hyperellipse and the portion of the SOC above it, thereby including the convex hull. There is freedom in choosing the hyperplane in step 2. It can be chosen to minimize its distance to the hull or in a way to minimize computation, as will be demonstrated in Section 4. In fact, solving (10) with respect to the vertices of the hull constitutes a possible solution but the complexity growth with the number of vertices renders it impractical for larger arrays.

4. TRAPEZOIDAL UNCERTAINTY MODELING

This section presents a general method to model the un-

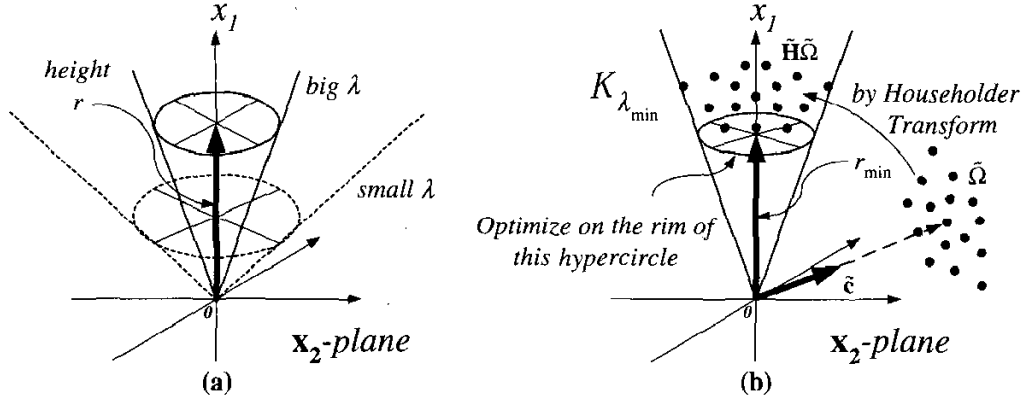


Fig. 3. (a) An upright SOC with variable cone angle. (b) Rotating $\tilde{\Omega}$ into the minimum bounding SOC.

certainties in the steering vector and demonstrates application of the proposed algorithm. Let $\mathbf{a} = [a_1 \cdots a_N]^T$. Referring to Fig. 2, an element a_i in \mathbf{a} may be subject to phase uncertainties α_i , β_i due to uncertain AOA, and phase and gain uncertainties, ψ_i , γ_i and δ_i , due to the amplifier. Thus a_i can assume any value inside the highlighted annulus sector in Fig. 2. A convenient way to encompass this sector is by a trapezoid with vertices a'_{i1} , a'_{i2} , a'_{i3} , a'_{i4} . Defining the vectors

$$\mathbf{a}'_k = [a'_{ik} \ a'_{2k} \ \cdots \ a'_{Nk}]^T \quad k = 1, 2, 3, 4 \quad (11)$$

whose normalized (unit-length) centroid is

$$\mathbf{c} = \frac{\sum_{k=1}^4 \mathbf{a}'_k}{\left\| \sum_{k=1}^4 \mathbf{a}'_k \right\|} \quad (12)$$

where $\|\cdot\|$ denotes the usual Euclidean vector norm, it can be seen that each element in the uncertain steering vector can be formed by a convex combination of the corresponding elements in these \mathbf{a}'_k 's. So the convex set Ω in (8) can be defined as the union of these points, i.e.,

$$\Omega = \left\{ [a'_{1k_i} \ a'_{2k_i} \ \cdots \ a'_{Nk_i}]^T \mid \begin{array}{l} k_i = 1, 2, 3 \text{ or } 4 \\ i = 1, 2, \dots, N \end{array} \right\} \quad (13)$$

It is not hard to verify that Ω is convex and every point in Ω constitutes a vertex of the minimum convex hull (of 4^N vertices) of Ω . Apparently, $\tilde{\Omega}$ is formed by stacking the real and imaginary parts of each point in Ω . Next, let's define a (convex) SOC of dimension $2N$ as

$$\mathcal{K}_\lambda \triangleq \left\{ \begin{bmatrix} x_1 \\ \mathbf{x}_2 \end{bmatrix} \mid x_1, \lambda \in \mathfrak{R}, \mathbf{x}_2 \in \mathfrak{R}^{2N-1}, x_1 \geq \lambda \|\mathbf{x}_2\| \right\} \quad (14)$$

As in Fig. 3(a), λ is a parameter that controls the cone angle with a large λ giving rise to a narrow cone and vice versa. All points in $\tilde{\Omega}$ are then rotated into the orientation of the SOC to find the tightest SOC that just contains the rotated $\tilde{\Omega}$ [Fig. 3(b)]. The Householder transform $\tilde{\mathbf{H}}$ can

conveniently rotate the point aggregate to an arbitrary direction (e.g., [2]). In our example the unit-vector along the SOC symmetry axis, $\tilde{\mathbf{z}} = [1 \ 0 \ \cdots \ 0]^T \in \mathfrak{R}^{2N}$, is chosen as the reference. Defining $\tilde{\mathbf{c}} = [\text{Re}(\mathbf{c})^T \ \text{Im}(\mathbf{c})^T]^T$,

$$\tilde{\mathbf{H}} = \begin{cases} \mathbf{I} - 2 \frac{(\tilde{\mathbf{c}} - \tilde{\mathbf{z}})(\tilde{\mathbf{c}} - \tilde{\mathbf{z}})^T}{(\tilde{\mathbf{c}} - \tilde{\mathbf{z}})^T (\tilde{\mathbf{c}} - \tilde{\mathbf{z}})}, & \tilde{\mathbf{c}} \neq \tilde{\mathbf{z}} \\ \mathbf{I}, & \tilde{\mathbf{c}} = \tilde{\mathbf{z}} \end{cases} \quad (15)$$

where $\tilde{\mathbf{H}}^{-1} = \tilde{\mathbf{H}}^T = \tilde{\mathbf{H}}$. Due to the structure of $\tilde{\Omega}$, the hyperellipte in step 3 (Section 3) of the proposed algorithm is a hypercircle tangent to the bottom of $\tilde{\mathbf{H}}\tilde{\Omega}$ at a height of r_{\min} , as in Fig. 3(b). To limit the length of this paper, the following facts are given without further elaboration: 1. Choosing $\tilde{\mathbf{c}}$, instead of other reference direction for $\tilde{\Omega}$, is due to its simple computation and the nearly-optimal $K_{\lambda_{\min}}$ that it gives; 2. r_{\min} can be obtained by the projection (a real value) of a point in Ω [wherein k_i is either 1 or 2 in (13)] onto \mathbf{c} ; 3. λ_{\min} can be obtained in $N-1$ comparison steps (As a reference, it requires $4N$ comparisons to obtain the radius of the smallest hypersphere in [1] bounding the annulus sector in Fig. 2).

Now, as described in step 4 of the proposed algorithm, optimization is performed on the hypercircle

$$\begin{bmatrix} r_{\min} \\ \tilde{\mathbf{d}}_z \end{bmatrix} \in K_{\lambda_{\min}} \quad \text{where } \tilde{\mathbf{d}}_z \in \mathfrak{R}^{2N-1}, \|\tilde{\mathbf{d}}_z\| = \frac{r_{\min}}{\lambda_{\min}} \quad (16)$$

Noting $\tilde{\Omega} = \tilde{\mathbf{H}}(\tilde{\mathbf{H}}\tilde{\Omega})$, the gain constraint in (10) becomes

$$\tilde{\mathbf{w}}^T (\tilde{\mathbf{H}} \begin{bmatrix} r_{\min} \\ \tilde{\mathbf{d}}_z \end{bmatrix}) \geq 1 \quad (17)$$

Let $\tilde{\mathbf{H}}_1$ be the first row in $\tilde{\mathbf{H}}$ and $\tilde{\mathbf{H}}_2$ be $\tilde{\mathbf{H}}$ without the first row, (17) can be rewritten as

$$-\tilde{\mathbf{d}}_z^T \tilde{\mathbf{H}}_2 \tilde{\mathbf{w}} \leq \tilde{\mathbf{H}}_1 \tilde{\mathbf{w}} - 1 \quad (18)$$

The maximum of the left hand side of (18) is achieved when $\tilde{\mathbf{d}}_z = -(r_{\min} / \lambda_{\min}) \tilde{\mathbf{H}}_2 \tilde{\mathbf{w}} / \|\tilde{\mathbf{H}}_2 \tilde{\mathbf{w}}\|$. So by introducing

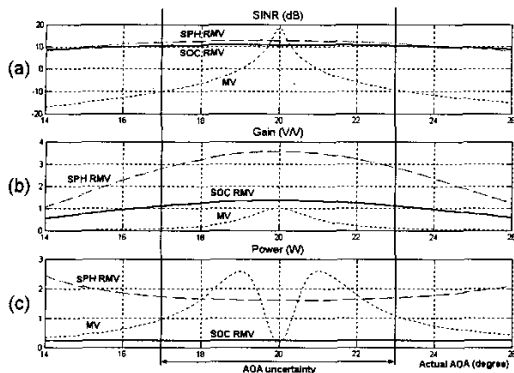


Fig. 4(a)-(c). Results of the Capon MV beamformer (MV), hypersphere beamformer (SPH RMV) and the proposed beamformer (SOC RMV) against AOA.

an auxiliary variable ε , and letting $\tilde{\mathbf{R}}_x = \tilde{\mathbf{U}}^T \tilde{\mathbf{U}}$ be the Cholesky factorization of $\tilde{\mathbf{R}}_x$, (10) is equivalent to:

$$\min(\varepsilon) \text{ subject to} \quad (19)$$

$$\|\tilde{\mathbf{U}}\tilde{\mathbf{w}}\| \leq \varepsilon \text{ and } \frac{r_{\min}}{\lambda_{\min}} \|\tilde{\mathbf{H}}_2 \tilde{\mathbf{w}}\| \leq \tilde{\mathbf{H}}_1 \tilde{\mathbf{w}} - 1$$

which is in the standard SOCP format [7], namely, minimizing a linear function over the intersection of an affine set and the product of SOCs. Efficient interior point algorithms [7]-[9] of worst-case iteration count bounded above by $O(\sqrt{N})$ can then be used to solve (19).

5. NUMERICAL EXAMPLES

Suppose three unit-power far-field signals are impinging on an 8-element uniform array separated by half wavelengths. Two of them are interference signals with AOAs 0° and 40° . The desired signal is coming from 20° with an uncertainty of $\pm 3^\circ$. For simplicity, all signals and the additive white Gaussian noise are assumed to be uncorrelated. The signal-to-noise ratio (SNR) is 10 dB. The steering vector elements all have a gain uncertainty of 0.05 and a phase uncertainty of 5° . The traditional MV, the hypersphere RMV and the proposed SOC RMV beamformers are compared and the results are as shown in Fig. 4. Using the public software in [9], the latter two SOCP problems are solved in generally less than 10 iterations (in fact, this is almost independent of the problem size). Fig. 4(a) shows the SINR for the three approaches, showing that there are tradeoffs in the peak SINR for the robust beamformers. It can be seen from Fig. 4(b) that the proposed SOC bounding method produces tighter results (gain ≥ 1) with respect to the specified range of uncertainty, while the hypersphere bounding method results in an "over-design" due to its inherent conservative nature. A major drawback of the hypersphere method is

the increased power consumption proportional to $\|\mathbf{w}\|^2$ ($= \|\tilde{\mathbf{w}}\|^2$) [6], illustrated in Fig. 4(c), that can cause the design to be practically infeasible. The proposed beamformer is superior since it always consumes a power comparable to the optimal value of the traditional Capon MV beamformer.

6. CONCLUSION

This paper has presented a geometrical approach for designing RMV beamformers using SOC bounding method. The algorithm exploits the convexity of the optimization constraint and reduces the dimension of the optimization process from a convex hull to the circumference of a hyperellipse. Its efficiency has been demonstrated through a general example of modeling array uncertainties using complex-plane trapezoids. The beamforming task has been transformed into an SOCP problem and efficiently solved using interior point algorithms. Numerical examples have confirmed the effectiveness, tightness and practicality of the proposed beamformer over other schemes.

7. REFERENCES

- [1] S.A. Vorobyov, A.B. Gershman and Z.Q. Luo, "Robust adaptive beamforming using worst-case performance optimization via second-order cone programming," *IEEE Int. Conf. on Acoustics, Speech, and Signal Processing*, vol. 3, pp. 2901-2904, May 2002.
- [2] S.Q. Wu and J.Y. Zhang, "A new robust beamforming method with antennae calibration errors," *IEEE Wireless Comm. and Networking Conf.*, vol. 2, pp. 869-872, Sep 1999.
- [3] A.B. Gershman, "Robust adaptive beamforming in sensor arrays," *AEU-Int. Journal Electron. Comm.*, vol. 53, no. 6, pp. 305-314, Dec 1999.
- [4] M. Wax and Y. Anu, "Performance analysis of the minimum variance beamformer in the presence of steering vector errors," *IEEE Trans. Signal Proc.*, vol. 44, no. 4, pp. 938-947, Apr 1996.
- [5] J. Capon, "High-resolution frequency-wavenumber spectrum analysis," *Proc. IEEE*, vol. 57, no. 8, pp. 1408-1418, Aug 1969.
- [6] F. Wang, V. Balakrishnan, P. Zhou, J. Chen, R. Yang and C. Frank, "Optimal array pattern synthesis using semidefinite programming," to appear in *IEEE Trans. Signal Processing*.
- [7] M. Lobo, L. Vandenberghe, S. Boyd and H. Lebet, "Applications of second-order cone programming," *Linear Algebra and its Applications*, 284:193-228, Nov 1998, Special Issue on Linear Algebra in Control, Signals and Image Processing.
- [8] Yu. Nesterov and A. Nemirovsky, *Interior Point Polynomial Algorithms in Convex Programming*, Society for Industrial and Applied Mathematics, Philadelphia, 1994.
- [9] J.F. Sturm, "Using SeDuMi 1.02, a MATLAB toolbox for optimization over symmetric cones," *Optim. Meth. Softw.*, vol. 11-12, pp. 625-653, Aug 1999.